Materials Science in Semiconductor Processing 39 (2015) 371–376

Contents lists available at ScienceDirect

Materials Science in Semiconductor Processing

journal homepage: www.elsevier.com/locate/mssp

Reactive pulsed laser deposited N–C codoped TiO_2 thin films

Inci Ruzybayev [a], Emre Yassitepe [b], Awais Ali [c], A.S. Bhatti [c], Reda Mohamedy Mohamed [d], Mohammad Islam [e], S.Ismat Shah [f,*]

[a] Department of Engineering and Computer Science, York College of Pennsylvania, York, PA 17403, United States
[b] Department of Materials Science and Engineering, University of Delaware, Newark, DE 19716, United States
[c] Centre for Micro and Nano Devices, Department of Physics, COMSATS Institute of Information Technology, Park Road, Islamabad 44000, Pakistan
[d] Chemistry Department, Faculty of Science, King Abdulaziz University, P.O. Box. 80203, Jeddah 21589, Saudi Arabia
[e] Center of Excellence for Research in Engineering Materials (CEREM), Advanced Manufacturing Institute, King Saud University, P.O. Box 800, Riyadh 11421, Saudi Arabia
[f] Department of Physics and Astronomy and Department of Material Science and Engineering, University of Delaware, Newark, DE 19716, United States

A B S T R A C T

TiO_2 is a large bandgap chemically stable oxide useful for several applications that involve photo-activated processes, including photocatalysis, photovoltaics, photoelectrolysis, etc. However, the large band gap renders this material not a very efficient absorber of the solar spectrum. Various schemes of cation and anion doping have been utilized that reduce this deficiency to a certain extent. In this paper we present the results of N–C codoping of TiO_2 thin films deposited by a reactive pulsed laser deposition technique. These films were compared for their optical and structural properties with undoped, N doped and C doped TiO_2 films prepared by the same technique. While all samples contained polycrystalline anatase phase, varying N_2 and CH_4 partial pressures resulted in change in TiO_2 lattice parameters due to codoping. X-ray diffraction high-resolution scans show the evidence of C incorporation into TiO_2 lattice by 2θ shift in (101) reflections due to large ionic radius of C. N doping was confirmed by XPS analyses. Direct relationship between oxygen vacancies and doping concentration was established by the deconvolution of XPS peaks. Considerable bandgap reduction occurred that was measured by using UV–vis diffuse reflectance spectroscopy. Results show that reactive pulsed laser deposition is indeed a useful method for the synthesis of codoped TiO_2 thin films as bandgap reduction of $\sim$1.00 eV via N–C codoping was successfully achieved.

1. Introduction

Since the discovery of the photocatalytic activity of TiO_2 in 1972 TiO_2 has been widely researched for applications in optoelectronics and catalysis [1]. However, due to the wide bandgap of TiO_2 (3.00–3.20 eV), the light absorption occurs in the UV range. Since solar spectrum consists of approximately 2% ultraviolet, 54% visible and 44% infrared wavelengths in AM 1.5, it is beneficial to increase the absorption to enhance TiO_2 activity under visible light. Therefore, bandgap tailoring is desired which can be achieved by modifying the electronic structure of TiO_2.

Previously, anion doping of anatase TiO_2 with C, N, F, P and S dopants was studied and the total density of states of the material as a result of substitutional doping was calculated [2]. N was the most promising dopant among all

* Corresponding author.
E-mail address: ismat@udel.edu (S.Isma. Shah).

http://dx.doi.org/10.1016/j.mssp.2015.05.013
1369-8001/

these anions since N 2p states overlap effectively with O 2p states with the possibility of forming a continuum of tail states in the bandgap causing an effective bandgap reduction. On the other hand, C dopant states did not overlap sufficiently with the edge states to help effective charge transfer. Another study pointed out that total dopant concentration is also important and must also be taken into account [3]. The actual mechanism of the bandgap reduction was studied to determine whether the visible light activity was due to substitutional doping [2], oxygen vacancies [4] or a combination of both [5].

The two relevant phases of TiO_2 are anatase and rutile. Although anatase phase has a slightly wider bandgap (3.20 eV) than rutile phase (3.00 eV), anatase is more efficient in terms of photocatalytic activity [6,7]. As mentioned earlier, the extent of dopant concentration also plays a role in effective bandgap reduction. There is a theoretical work done by Wang and Lewis which shows that the bandgap of anatase can be reduced more efficiently with higher dopant concentration of N and C, both at 5.20%, compared to lower dopant concentration at 0.52% of N and at 0.26% of C [3].

Previously, N doped anatase TiO_2 films were prepared in our group by a reactive pulsed laser deposition (RPLD) technique and their electronic structure was investigated [5,8]. XPS valence band scans showed that N 2p states were located just above O 2p states which is in agreement with Asahi [2]. In addition, N doping created oxygen vacancies [5,8]. As a result, effective optical bandgap reduction was observed as a function of the doping concentration. C doped anatase-rutile mixed TiO_2 films were also prepared by the same technique [9]. Bandgap was lowered slightly due to the presence of mixed phases rather than C doping. As Asahi stated, C dopant states create trap states [2] and C doping is not as efficient as N doping.

N–C codoping, on the other hand, could facilitate charge transfer since a mixture of C and N dopant states could lead to a continuum of impurity states close to the conduction band edge. In this study, we present the results of bandgap tailoring of TiO_2 by anion codoping. N–C codoped TiO_2 thin films were prepared by the reactive pulsed laser deposition (RPLD) to incorporate impurities that modify electronic structure of TiO_2 synergistically. PLD is known as a powerful technique for preparing thin films. Its advantages include simple setup [10], capability of depositing metastable materials due to high energy of the laser beam and the resulting ablated flux [11,12], stoichiometric transfer between target to substrate which is different from thermal evaporation and sputtering techniques [12], and reproducibility [10–13]. Using reactive gases during deposition makes PLD even more powerful since it is free of electron beams or hot filaments [12] that could interact with the reactive gases. RPLD also does not have sputtering-like target poisoning issues [14]. Easily controllable partial pressures of reactive gases allow a wide range of ratios of gases in the PLD chamber in order to control doping concentration. In this work we show that the bandgap of anatase TiO_2 is successfully lowered by $\sim$1.00 eV due to N–C codoping. A direct relationship between oxygen vacancy and doping concentration was observed. As the N dopant concentration increases (along with C incorporation), the bandgap of TiO_2 decreases [3,15].

Although N–C codoped TiO_2 samples have previously been prepared by using sol–gel [16,17], MOCVD [18], magnetron sputtering [19] and oxidative annealing of the titanium carbonitride compounds in air [20], this paper reports the results of the N–C codoped TiO_2 thin films synthesized by the RPLD method which is preferred owing to the advantages listed earlier. One of the most desirable applications of these thin films is as photoanode material in photoelectrochemical cells for solar hydrogen generation. Due to the aqueous environment of such cell it is imperative that there is good adhesion between the film and the substrate. PLD with high energy of the ablated flux provides a stronger thin film – substrate interface which makes it a better suited technique for the fabrication of photoanodes. A photoanode material for photoelectrolysis has to be able to split water and, therefore, the band gap of the semiconductor needs to be greater than 1.23 eV, which is the difference between redox potential of $H+/H_2$ and of O_2/H_2O. It should also be stable in an aqueous medium, cheap and non-toxic, and it should absorb most of the solar spectrum for maximum efficiency. TiO_2 satisfies all these requirements but the last one. While it is one of the most stable materials, the large band gap TiO_2 can absorb only the UV part of the solar spectrum.

This paper describes the study of N and C codoping of TiO_2 thin films with the goal to achieve a band gap reduction larger than what is achievable by individual doping with C or with N. For this purpose a series of undoped and N–C codoped (20N–80C and 80N–20C) TiO_2 samples were prepared to achieve the synergistic effect of N–C codoping in anatase thin films. N–C codoped TiO_2 thin film samples are labeled as *X*N–*Y*C, where *X* and *Y* are the partial pressures of N_2 and CH_4 gases, respectively. For example, 20N–80C refers to a sample deposited with 2.67 Pa N_2 and 10.67 Pa CH_4. We should note that only N doped TiO_2 [5,8] and only C doped TiO_2 [9] thin films have previously been prepared by the RPLD technique and studied in detail by our group and we refer to these works as necessary.

2. Experimental

TiO_2 thin film samples were prepared by using the RPLD technique. The details of the PLD system used to prepare TiO_2 thin films were published previously [13]. Briefly, a KrF excimer laser at constant energy of 450 mJ and pulse rate of 15 Hz was used for ablation. The laser pulse duration was 25 ns. Pure TiO_2 target was prepared by compressing and sintering titanium (IV) oxide (Sigma-Aldrich) powder at 800 °C for 6 h under Ar gas atmosphere that resulted in a polycrystalline anatase TiO_2 target. This preparation method was similar to the one utilized previously by our group [8]. The chamber was pumped down to a base pressure of 0.67 mPa using a turbo molecular pump backed by a mechanical pump. Target rotation was kept constant at 15 rpm. Indium-doped tin oxide (ITO) coated glass substrates were used for deposition. Substrates were cleaned with isopropyl alcohol in ultrasonic cleaner for 30 min and subsequently triple rinsed with deionized water and dried in dry nitrogen. Prior to deposition, substrate temperature was gradually increased to 600 °C by using two 500 W halogen

lamps placed directly underneath the substrate holder. The temperature was chosen so that anatase, rather than rutile phase, could be stabilized in the films. N_2 and CH_4 gases were used as reactive gases for the N and C dopants by admitting them into the chamber after the required system pressure and substrate temperature were established. Deposition time for all samples was kept constant at 20 min. For the undoped TiO_2 samples, only oxygen gas was admitted in the deposition chamber and the pressure was kept constant at 13.33 Pa throughout the deposition. For the codoped samples, chamber pressure during the deposition was still kept constant at 13.33 Pa by introducing a mixture of N_2 and CH_4 reactive gases. No oxygen gas was admitted in this case. Partial pressures of N_2 and CH_4 were adjusted to achieve the desired composition of the gas mixture. Chamber pressure was set at 13.33 Pa as above this pressure the turbo-pump performance is compromised.

X-ray diffraction (XRD) data was obtained using Rigaku D-Max B diffractometer equipped with a graphite crystal monochromator and a Cu Kα radiation source ($\lambda = 1.5405$ Å). XRD scans were performed at 30 kV and 30 mA. Bragg reflections from crystal planes for survey scan of each sample was collected in the range of $2\theta = 20^\circ$ and 70° with a step size of 0.02° and collection time of 2 s per step. Step size for high-resolution scans were decreased to 0.002°. WinJade software (Materials Data Inc. Livermore, CA) was used for XRD pattern analyses.

Omicron EA125 X-ray photoelectron spectroscopy (XPS) system was used to determine the chemical structure and composition of the thin films. Non-monochromatic Al X-rays (1486.5 eV) were employed in association with CasaXPS software for the deconvolution of the peaks and quantifications were carried out by using C 1s peak related to the C–C bond located at 284.5 eV as reference peak. Pass energy ranged between 50 eV for survey scans and 25 eV for high-resolution scans. Quantifications were done using high-resolution XPS scans.

Optoelectronic measurements were carried out by using a Perkin-Elmer Lambda 35 UV–vis spectrometer equipped with an integrating sphere. UV–vis diffuse reflectance spectroscopy (DRS) technique was used to obtain transmittance (T), diffuse reflectance (R) and absorbance (A) spectra. Absorption coefficient of each sample was calculated by using the following equation:

$$\alpha = -\frac{1}{d}\ln\left(\frac{T}{(1-R)^2}\right) \quad (1)$$

where α is the absorption coefficient and d is the thickness of the sample. Using absorption coefficient and corresponding energy in the range of 1.60–4.80 eV, the indirect bandgap of each sample was determined by the Tauc equation as follows:

$$\alpha \propto \frac{(h\nu - E_{gap})^2}{h\nu} \quad (2)$$

By plotting $h\nu$ vs. $\sqrt{\alpha h\nu}$ and extrapolating linear part to zero, the approximate value for bandgap can be obtained [21,22]. The bandgap of undoped TiO_2 was measured to be ~3.20 eV which is the generally accepted value for the bandgap of bulk anatase in literature [23,24].

3. Results and discussion

Typical XRD patterns of undoped TiO_2, 20N–80C and 80N–20C samples are shown in Fig. 1(a). The XRD patterns show that all samples deposited at 600 °C substrate temperature and 13.33 Pa ablation pressure are polycrystalline anatase phase (A). Additional peaks in the XRD patterns are the ITO related peaks emanating from the substrate. Previous work on PLD deposited N doped TiO_2

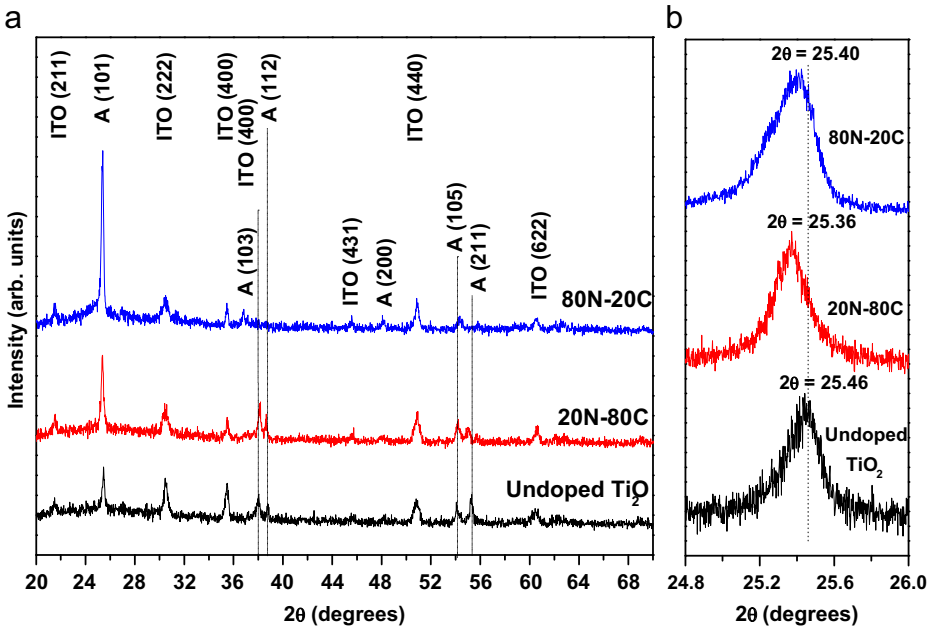

Fig. 1. (a) XRD survey scans and (b) HR-XRD scans of thin film samples.

showed that the films were also in anatase structure [8] whereas XRD results of PLD study on C doping showed presence of mixed rutile and anatase phases, even though anatase phase was still dominant [9]. It is important to note that the difference between these previous works on N doped and C doped TiO_2 samples and this work is that the precursors for N and C are the reactive gases. N doped samples were prepared under the mixture of O_2/Ar and N_2 gases [19] while C doped samples were prepared under the mixture of O_2/Ar and CH_4 gases [20]. Thus, different dopant concentrations were obtained. 13.3 Pa total deposition pressure was constant for all compared samples. The results on the effect of oxygen partial pressure on N–C codoped TiO_2 thin films were presented in another study [25]. Anatase to rutile transition was observed with the decreasing oxygen pressure. This is most probably due to the creation of oxygen vacancies which eventually cause collapse of the structure to a denser rutile (4.2–4.3 g/cm^3) compared to anatase (3.8–3.9 g/cm^3) as has previously been observed by Lin et. al. [8].

Anatase related peaks were identified using Joint Committee on Powder Diffraction Standards (JCPDS) card #841285. XRD patterns of codoped films varied, depending on the partial pressure of the N_2 and CH_4 reactive gases, as compared to undoped films in which we used 13.33 Pa pure O_2 gas pressure. Fig. 1(b) shows the high-resolution XRD (HR-XRD) scans focusing on the 2θ shifts in the main anatase peak, A (101). From the WinJade analysis, 2θ positions and corresponding FWHM of the A (1 0 1) of undoped TiO_2, 20N–80C and 80N–20C samples were found to be at 25.46° (FWHM: 0.1773), 25.36° (FWHM: 0.1767) and 25.40° (FWHM: 0.2487). The shifts in the A (101) peak of codoped samples compared to undoped TiO_2 are due to the incorporation of N and C dopants into the anatase TiO_2 lattice. C^{-4} ionic radius (2.60 Å) is much larger than the ionic radius of both N^{-3} (1.71 Å) and O^{-2} (1.40 Å) anions. Therefore, the 2θ shift in 20N–80C is larger than the shift in 80N–20C, due to higher C to N ratio obtained by altering relative partial pressures of CH_4 and N_2 gases.

XPS measurements were carried out in order to examine the changes in the composition and the electronic structure of the thin films. Direct correlation between N_2 partial pressure and N dopant concentration was established from the analysis of N 1s region high-resolution scans. Due to high concentration of adventitious C on the surface of the thin films, the evidence of Ti–C bond related to substitutional C doping is not conclusive. The C 1s binding energy for Ti–C bond in C doped anatase structure is 280.5 eV and it is an indication of the substitutional C doping in TiO_2 [26]. Chen and coworkers studied C and N codoped TiO_2 nanoparticles synthesized at 400 °C and 500 °C by using the sol–gel method [16]. Neither their N–C codoped TiO_2 samples prepared by sol–gel [16], nor only C doped TiO_2 films prepared by PLD [9] show Ti–C related peak in the C 1s high-resolution scans. XPS is a surface sensitive technique and, therefore, etching can be used to remove the surface contamination due to adventitious C. For example, Hsu and coworkers investigated C-doped TiO_2 films with a range of C concentration from 0.8 to 1.3 mol% and showed that a depth profile was necessary to reveal the peak related to the Ti–C bond which is the evidence of substitutional C doping [27]. However, in that work the intensity of the peak related to Ti–C bond was increasing with etching time and so did the C dopant concentration. Etching is not the only way to show that there is indeed C incorporation into the TiO_2 lattice. XRD, for example, is not surface limited and 2θ shift in A (101) peak of codoped samples changes with partial pressures of N_2 and CH_4 gases, as mentioned earlier, which is a direct result of C (and N) substitution in TiO_2 lattice. Likewise, bandgap measurements from UV–vis DRS measurements illustrate the effect of substitutional codoping.

Quantification of the XPS data using high-resolution scans was carried out by taking into consideration four regions: C 1s, N 1s, O 1s and Ti $2p_{3/2}$. Undoped TiO_2 did not show any N related peaks. Adventitious carbon, however, was recorded in C 1s region. Atomic concentrations were calculated by using atomic sensitivity factor of C 1s (0.297), N 1s (0.477), O 1s (0.711) and Ti $2p_{3/2}$ (1.334) [28]. As mentioned earlier, 20N–80C samples were prepared under 2.67 Pa N_2 and 10.67 Pa CH_4, while 80N–20C samples were prepared under 10.67 Pa N_2 and 2.67 Pa CH_4. Although, C 1s region calculations do not reflect the precise concentrations of C as substitutional dopant due to the presence of adventitious carbon on each sample, corrections were made by subtracting adventitious carbon value obtained in undoped TiO_2 from carbon values of codoped samples. Thus, the relation between estimated C concentrations and CH_4 partial pressure is shown. While CH_4 partial pressure decreased from 10.67 to 2.6 Pa, C concentration also decreased from 10.95% to 0.66%. In contrast to C doping, substitutional N doping is easy to identify from XPS and significant amount of substitutional N was observed as shown in the high-resolution scans of N 1s region in Fig. 2.

N is more electronegative than C. In Pauling units the values are 3.04 and 2.55 [29]. It is easier to form Ti–N bonds than to form Ti–C bonds. Therefore, N substitutional doping is more favorable. Under oxygen deficient conditions substitutional N [30] and substitutional C doping [31] is favorable with oxygen vacancies. N peak at 395.90 eV corresponds to the substitutional doping [8,17,32]. As the N_2 partial pressure increases from 2.66 Pa (as in 20N–80C in mTorr) to 10.67 Pa (as in 80N–20C), the substitutional N concentration increases from 1.54% to 5.01%. Our substitutional N peak position value at 395.49 eV for 20N–80C and 395.52 eV for 80N–20C eV is in agreement with the literature value given above. With the increasing partial pressure of N_2 gas substitutional N doping can be increased, as previously reported [33].

Further analyses were performed to show the relationship between N doping concentration and oxygen vacancies using Ti 2p high-resolution XPS spectra shown in Fig. 3. Deconvolution of peaks in Ti 2p region shows four peaks in the codoped thin films; Ti^{4+} and Ti^{3+} associated with Ti $2p_{1/2}$ and Ti $2p_{3/2}$. For 80N–20C, 20N–80C and undoped TiO_2 samples, Ti^{4+} peak is at 457.89 eV, 458.28 eV and 458.36 eV, respectively. The shoulder at a lower binding energy on the Ti $2p_{3/2}$ peak corresponds to the oxygen vacancies (Ti^{3+} states) [15,34]. Ti^{3+} peak is located at 456.19 eV for 80N–20C and 456.78 eV for 20N–80C. The FWHM values were kept constant. The direct relationship between the oxygen vacancies and the

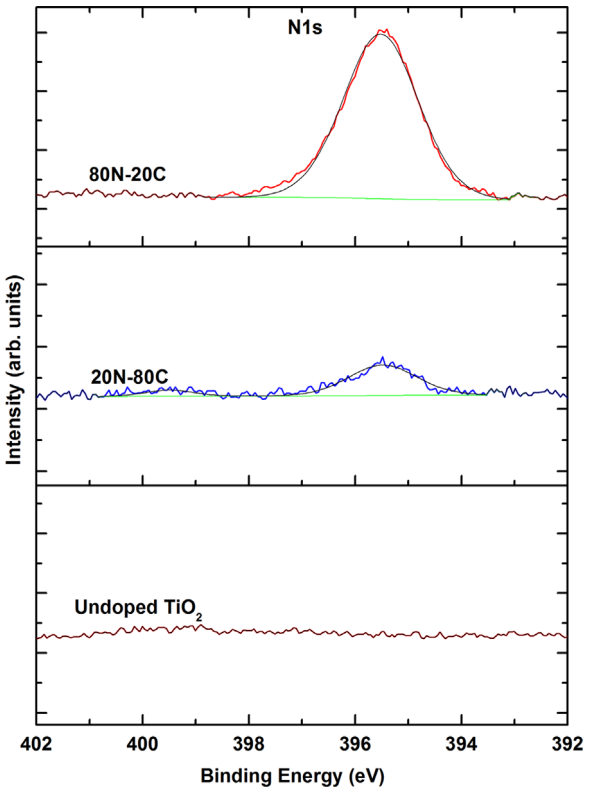

Fig. 2. N 1s high-resolution XPS spectra. Note that increasing partial pressure of N_2 reactive gas results in increasing N dopant concentration.

substitutional dopant concentration has previously been reported in the literature [5,33,35–37]. Computational calculations done by Di Valentine and co-workers showed that oxygen vacancy formation energy reduces from 4.2 eV to 0.6 eV in the presence of N doping [37]. The shoulder (Ti^{3+}) intensity increases with increasing N doping concentration. Moreover, the Ti^{4+} peak shifts towards lower binding energy which is attributed to the chemical potential shift due to defects [38]. Another indication of oxygen vacancies can be found by investigating positions of Ti 2p doublet. Doublet separation increases as Ti reduces from Ti^{4+} to Ti^{0} [28]. The values were measured for undoped TiO_2, 20N–80C and 80N–20C are 5.75 eV, 5.77 eV and 5.87 eV, respectively.

Transmittance, reflectance and absorbance measurements were done using Perkin-Elmer UV–vis DRS. The bandgap was estimated from plotting $h\nu$ vs. $\sqrt{\alpha h\nu}$ by the extrapolation of the straight line to the point where α becomes zero, as shown in Fig. 4. Inset of Fig. 4 is the transmittance plot and the films are about 50% transparent to visible light. The bandgap of undoped TiO_2 thin films was found to be ~3.20 eV. Codoping of TiO_2 with N and C reduced the bandgap successfully to ~2.50 eV and ~2.20 eV for 20N–80C with 1.54% substitutional N and for 80N–20C with 5.01% substitutional N, respectively.

Although it was not possible to calculate the concentration of substitutional C doping with high confidence level with the techniques we used, bandgap of 20N–80C, which has the highest C concentration among all, was successfully lowered as compared to the bandgap of undoped TiO_2 by ~0.70 eV. Only C doped TiO_2 thin film reduced the bandgap to 3.15 eV from 3.25 eV, as previously reported [9]. Since 20N–80C also contains N doping (1.54%), one may argue that the reason for the reduction is due to N doping. However, N-doped TiO_2 thin films prepared by PLD method showed that 4.40% N concentration reduces the bandgap of N-doped TiO_2 thin films by 0.77 eV [8]. Hence, the reduction of the bandgap was due to the codoping with N and C; possibly forming continuous doping states within the forbidden region and overlapping

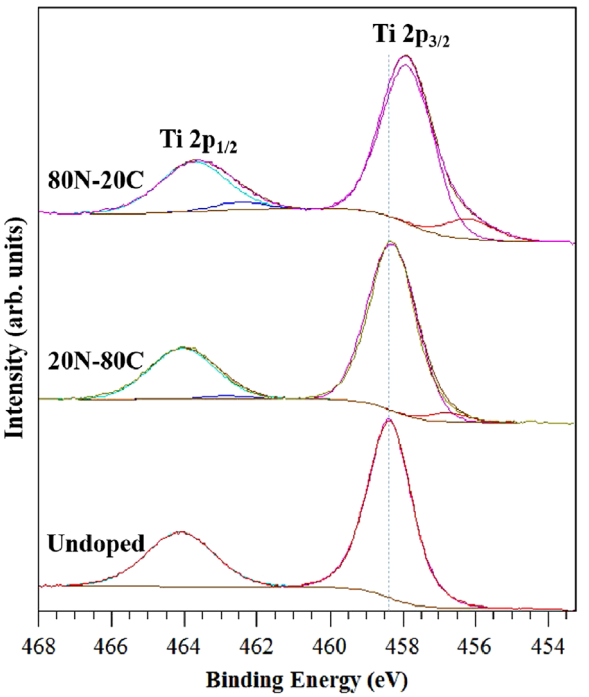

Fig. 3. Ti 2p region high-resolution XPS scans of the undoped and doped samples.

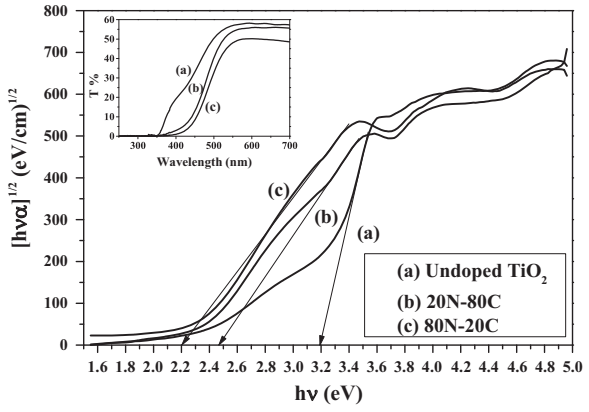

Fig. 4. Bandgap estimation of undoped and N–C codoped samples from UV–vis DRS. Transmittance plot is given as inset. The extrapolation of linear part of the curve presents the approximate values for bandgap which are (a) undoped TiO_2, ~3.20 eV, (b) 20N–80C, ~2.50 eV and (c) 80N–20C, ~2.20 eV.

with O 2p states. Similar argument applies to 80N–20C thin film samples that had the lowest bandgap, ~2.20 eV. Higher N dopant (5.01%) film, 80N–20C, resulted in narrower bandgap than higher C dopant film, 20N–80C.

4. Summary and conclusions

Reactive pulsed laser deposition technique was used to prepare N–C codoped TiO_2 thin films at 600 °C and under 13.2 Pa total gas pressure. Two codoped samples, 20N–80C and 80N–20C, were compared with undoped, N doped and C doped TiO_2 samples. Deposition pressure was kept constant at 13.33 Pa by adjusting N_2 and CH_4 partial gas pressures for N–C codoped films. XRD scans show polycrystalline anatase TiO_2. The shift in A (101) main peak towards the smaller 2θ indicates a strain effect due to incorporation of dopants into TiO_2 lattice. Since C has a larger ionic radius than N and O, 20N–80C sample which has the higher C doping presents a greater shift. XPS results clearly shows substitutional N doping from N 1s high-resolution scans. As expected, substitutional doping amount increases with increasing N_2 gas partial pressure. Reduced Ti (Ti^{3+}) is an indication of oxygen vacancies and 80N–20C had a larger Ti^{3+} shoulder and a greater Ti 2p doublet separation. Therefore, increased N concentration results in more oxygen vacancies in codoped samples. Note that while N concentration increases C concentration decreases. Considerable bandgap reduction was measured by using UV–vis DRS due to N–C codoping. While C abundant codoped film, 20N–80C, had a bandgap of ~2.50 eV, N abundant codoped film, 80N–20C, had ~2.20 eV bandgap. As compared to C doped and N doped films, N–C codoping present much lower bandgap reduction due to synergetic effect of codoping. That is, the continuum defect states may be formed overlapping effectively with O 2p states at the valence band maximum. In codoped samples N effect is more pronounced in terms of bandgap reduction. However, C extends the defect states within the bandgap and contributes to a greater reduction of bandgap. We show that N–C codoped TiO_2 films prepared by RPLD technique have lower bandgap than N doped and C doped TiO_2. Therefore, N–C codoped films are better choice for applications using visible light irradiation. With the RPLD technique, doping concentrations was easily varied and metastable films were obtained.

References

[1] A. Fujishima, K. Honda, Nature 238 (1972) 37–38.
[2] R. Asahi, T. Morikawa, T. Ohwaki, K. Aoki, Y. Taga, Science 293 (2001) 269–271.
[3] H. Wang, J.P. Lewis, J. Phys. Condens. Matter 18 (2006) 421–434.
[4] N. Serpone, J. Phys. Chem. B 110 (2006) 24287–24293.
[5] A.K. Rumaiz, J.C. Woicik, E. Cockayne, H.Y. Lin, G.H. Jaffari, S. Ismat Shah, Appl. Phys. Lett. 95 (2009) 262111–262113.
[6] A. Sclafani, L. Palmisano, E. Davi, J. Photochem. Photobiol. A Chem. 56 (1991) 113–123.
[7] A. Vidal, J. Herrero, M. Romero, B. Sanchez, B. Sanchez, J. Photochem. Photobiol. A Chem. 79 (1994) 213–219.
[8] H. Lin, A.K. Rumaiz, M. Schulz, C.P. Huang, S.I. Shah, J. Appl. Phys. 107 (2010) 1243051–1243056.
[9] B. Zhou, M. Schulz, H.Y. Lin, S.I. Shah, J. Qu, C.P. Huang, Appl. Catal. B Environ. 92 (2009) 41–49.
[10] Y. Suda, H. Kawasaki, T. Ueda, T. Ohshima, Thin Solid Films 475 (2005) 337–341.
[11] G. Soto, Appl. Surf. Sci. 233 (2004) 115–122.
[12] D.H. Lowndes, D.B. Geohegan, A.A. Puretzky, D.P. Norton, C. M. Rouleau, Science 273 (1996) 898–903.
[13] H. Lin, A.K. Rumaiz, M. Schulz, D. Wang, R. Rock, C.P. Huang, et al., Mater. Sci. Eng. B 151 (2008) 133–139.
[14] D. Guerin, S.Ismat Shah, J. Vac. Sci. Technol. A Vac. Surf. Film 15 (1997) 712–715.
[15] Y.-P. Peng, E. Yassitepe, Y.-T. Yeh, I. Ruzybayev, S.I. Shah, C.P. Huang, Appl. Catal. B Environ. 125 (2012) 465–472.
[16] D. Chen, Z. Jiang, J. Geng, Q. Wang, D. Yang, Ind. Eng. Chem. Res. 46 (2007) 2741–2746.
[17] J. Yang, H. Bai, Q. Jiang, J. Lian, Thin Solid Films 516 (2008) 1736–1742 .
[18] Y.-H. Tseng, C.-S. Kuo, C.-H. Huang, Y.-Y. Li, Z. Phys. Chem. 224 (2010) 843–856.
[19] K.R. Wu, C.W. Yeh, C.H. Hung, C.Y. Chung, L.H. Cheng, J. Nanosci. Nanotechnol. 10 (2010) 1057–1064.
[20] C. Yu, J.C. Yu, Catal. Lett. 129 (2009) 462–470.
[21] J.I. Pankove, Optical Processes in Semiconductors, Dover Publications, NY, 1971.
[22] W.M. Yim, E.J. Stofko, P.J. Zanzucchi, J.I. Pankove, M. Ettenberg, S. L. Gilbert, Physics 44 (1973) 292–296.
[23] N. Daude, C. Gout, C. Jouanin, Phys. Rev. B 15 (1977) 3229–3235.
[24] L. Zhao, Q. Jiang, J. Lian, Appl. Surf. Sci. 254 (2008) 4620–4625.
[25] I. Ruzybayev, S.I. Shah, Surf. Coat. Technol. 241 (2014) 148–153.
[26] H. Irie, Y. Watanabe, K. Hashimoto, Chem. Lett. 32 (2003) 772–773.
[27] S.-W. Hsu, T.-S. Yang, T.-K. Chen, M.-S. Wong, Thin Solid Films 515 (2007) 3521–3526.
[28] J.F. Moulder, W.F. Stickle, P.E. Sobol, K.D. Bomben, Handbook of X-Ray Photoelectron Spectroscopy, 1995.
[29] G. Liu, L. Wang, H.G. Yang, H.-M. Cheng, G.Q. (Max) Lu, J. Mater. Chem. 20 (2010) 831–843.
[30] E. Finazzi, C. Di Valentin, J. Phys. Chem. C 2 (2007) 9275–9282.
[31] C. Di Valentin, G. Pacchioni, A. Selloni, Chem. Mater. 17 (2005) 6656–6665.
[32] T. Morikawa, R. Asahi, T. Ohwaki, K. Aoki, Y. Taga, Jpn. J. Appl. Phys. 40 (2001) 561–563.
[33] M. Kitano, K. Funatsu, M. Matsuoka, M. Ueshima, M. Anpo, J. Phys. Chem. B 110 (2006) 25266–25272.
[34] A.K. Rumaiz, B. Ali, A. Ceylan, M. Boggs, T. Beebe, S. Ismat Shah, Solid State Commun. 144 (2007) 334–338.
[35] H. Lin, Improving the optoelectronic property and photoactivity of nanostructured titanium dioxide: effect of particle size, oxygen vacancy, and nitrogen doping Ph.D. thesis, University of Delaware, Newark, DE, 2008.
[36] I. Takahashi, D.J. Payne, R.G. Palgrave, R.G. Egdell, Chem. Phys. Lett. 454 (2008) 314–317.
[37] C. Di Valentin, G. Pacchioni, A. Selloni, S. Livraghi, E. Giamello, J. Phys. Chem. B 109 (2005) 11414–11419.
[38] N.C. Saha, H.G. Tompkins, J. Appl. Phys. 72 (1992) 3072–3079.